NGST Science and Technology Exposition
ASP Conference Series, Vol. 207, 2000
E. P. Smith, and K. S. Long, eds.

MIRCAM: Mid-Infrared Wide Field Camera for NGST

Winfried Posselt

Dornier Satellitensysteme, Ottobrunn, Germany

Gillian Wright

Astronomy Technology Centre, Edinburgh, UK

Pierre-Olivier Lagage

SAp CEA-Saclay, France

Olivier Le Fèvre

Laboratoire d'Astronomie Spatiale, Marseille, France

Abstract.

NASA has invited ESA to extend their successful collaboration on HST to the NGST project, and ESA has undertaken a number of assessment studies which aimed at defining its potential instrument and spacecraft hardware contributions to the NGST mission. One of these ESA studies called "Study of Payload Suite and Telescope for NGST" (ESTEC/Contract No. 13111/98/NL/MS), has been conducted by Dornier Satellitensysteme (DSS), together with Alcatel Space (AS), and a team of 16 European science institutes chaired by Laboratoire d'Astronomie Spatiale (LAS) and UK Astronomy Technology Centre (UK-ATC). DSS took the responsibility for the overall study and the payload, AS for the telescope, and the science team was responsible for the instrument and telescope definition and requirements.

The MIRCAM is one out of four instruments that were defined by the science team as potential NGST payload and were detailed by DSS. This document discusses the optical and opto-mechanical design and analyses of the instrument. Technical aspects that are common to instruments studied by DSS are described in separate reports ("NGST Payload Study, Final Report" and Posselt, et al. 2000).

1. Introduction

Mid-IR camera and spectrograph capabilities are essential for 3 of the 7 core programs identified in the NASA design reference mission. The key reasons why mid-IR capabilities covering the 5–28 μm band will be important for the NGST are: (i) The mid-IR provides truly unique diagnostics and is unexplored at the spatial resolution and sensitivity NGST will be capable of. Thus there

is great potential for serendipitous science. (ii) Without observing the universe above 10 μm, NGST would miss star formation history, since ISO and sub-mm data indicate that even at high red-shifts most of the star-formation is dust enshrouded and the UV-optical tells only part of the story. Mid-IR observations out to 28 μm on NGST would enable the identification of the galaxies responsible for the IR background through their dust emission up to $z = 3.8$ for 10^{11} $L_{\odot}$ galaxies and $z = 8$ for brighter ones. (iii) Formation of stars and planetary systems occurs deep in molecular clouds, $A_v > 100$, so can only be probed at > 10 μm. Diffraction limited observations at 10 μm will spatially resolve planet formation via holes in proto-planetary disks to distances of 200 pc. (SIRTF will provide large samples). ISO has shown the diagnostic value of mid-IR spectroscopy for solid material condensing during planet formation. (iv) ISO results show that most of the star-formation in interacting and merging galaxies is deeply embedded in dust. Mid-IR dust features and fine structure lines (at > 10 μm) are essential to separate starburst and AGN as the power source in obscured galaxies. This study of physics of starbursts and AGN is central to our understanding of galaxy formation and evolution.

2. Science Specifications

The mid-IR science goals call for both high resolution imaging with as wide a field as practicable, and for moderate resolution spectroscopy. Instruments which combine imaging and integral field spectroscopy with the same arrays used for either mode are possible, but this requires a mechanism. We gave a high importance to simplicity, and so chose to have camera and spectrograph modules which are independent optically and use separate arrays. The camera has two channels and these were again designed as optically independent modules. The range of modules explores the possibilities for the mid-IR for different numbers of arrays and allows for descope/further simplification.

For the camera the goal was to able to observe simultaneously in two channels to maximize survey efficiency. The selection of pixel scale is a difficult choice requiring a balance between field and sampling of images. An adjustable plate scale requires a mechanism and it is simpler to use different spatial sampling in each channel. Since NGST will be capable of uniquely high spatial resolution in the mid-IR compared to other space missions, we chose to emphasize fully sampling the diffraction limited spot at the short wavelengths of each camera band. Based on these decisions the requirements for the mid-IR camera were finalized to be as given in Table 1.

3. Optical Design and Analyses

In order to achieve the required simultaneous observations in two spectral bands the MIRCAM is set up of two optical modules:

- MIRCAM-SW for the short wavelength range (5 to 10 μm)
- MIRCAM-LW for the long wavelength range (10 to 28 μm)

Table 1. MIRCAM High Level Specifications

Item	Specification
Wavelength Range	Two channels: 5–10 μm, 10–28 μm
Field of View	2.5 × 2.5 arcmin
Spatial sampling	0.075 arcsec/pixel (5–10 μm) 0.15 arcsec/pixel (10–28 μm)

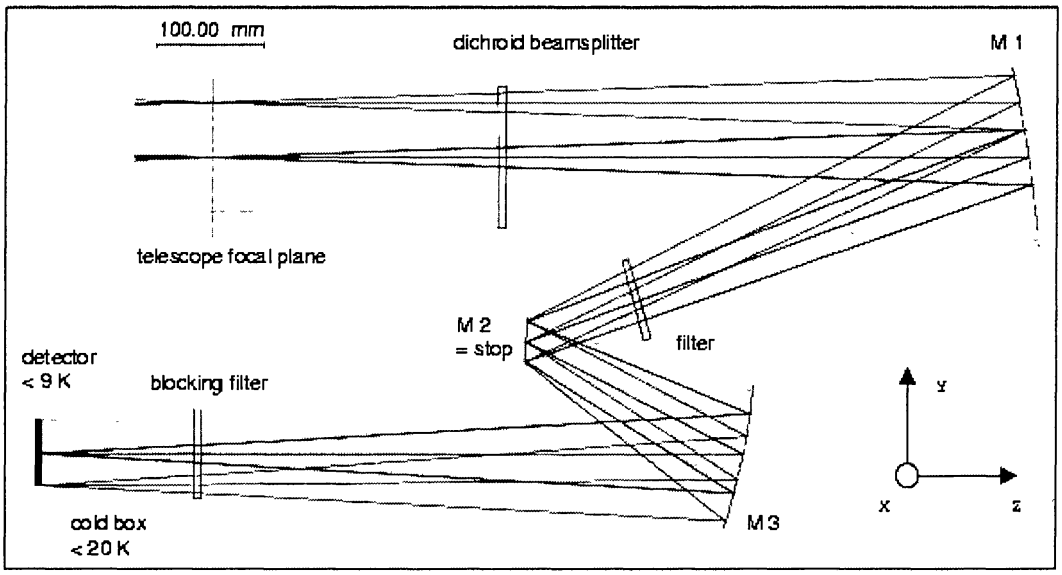

Figure 1. Optical configuration of MIRCAM-SW.

Both cameras have the same optical design principle. They are relay optics with different reduction ratios, that image the telescope focal plane onto the detector array. The different reduction ratios adapt the required different spatial resolutions to the same detector pixel sizes (the same Si:As detector arrays are foreseen for both instruments (see "NGST Payload Study, General Design Considerations," these proceedings). The wavelength split at 10 μm is performed by a dichroic beam-splitter which transmits the short and reflects the long wavelengths. Proposed substrate material is ZnSe.

3.1. Optical Design of SW Channel

The optical configuration of MIRCAM-SW is based on the requirements of Table 1 and shown in Figure 1. It is an all-reflective design with a telecentric entrance pupil and a reduction ratio of 1.5.

The optics is a 3 mirror system (M1, M2 and M3). The front focal plane of M1 is adjusted to the telescope focal plane, resulting in a quasi-parallel beam

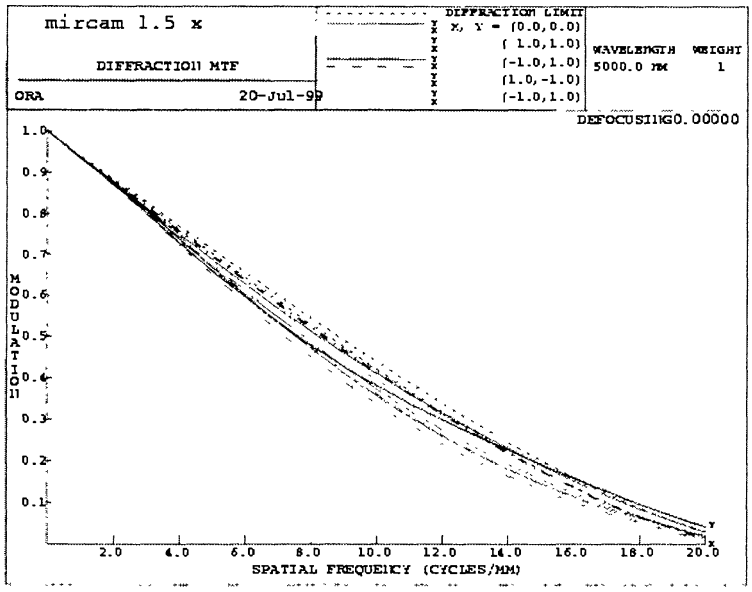

Figure 2. MIRCAM-SW: MTF as a function of spatial frequency calculated in center and corners of the field.

(divergence < 30 mrad) between M1 and M2. This is a suitable location for the filter wheel. M1 images the telecentric entrance pupil on its back focal plane, where M2 is located. In this way, the physical shape of M2 defines the aperture stop of the camera. M2 and M3 re-image the telescope focal plane onto the detector. The M1 surface is conical decentered and M2, M3 are spherical decentered. The conic design is not critical with respect to manufacturing. The SW channel design parameters are listed in Table 2.

The broad band filters are accommodated on a filter wheel, which is located in the parallel beam close to the pupil stop. Blocking filters on one or two substrates in front of the detector array block the wavelengths below 5 μm and above 10 μm. In the present design, there is one filter under an angle of about 36° to avoid ghost images. The detector array is cooled to a temperature < 10 K. The correct focusing on the image can be achieved by adjusting the detector array.

The optics have been optimized including the dichroic beam-splitter and blocking filter. The optical performance of the camera is diffraction limited. The Strehl ratios exceed 0.89 across the whole field. The MTF as a function of frequency is given in Figure 2. The field angles are expressed in relative coordinates w.r.t. the maximum field angles.

3.2. Optical Design of LW Channel

The optical configuration of MIRCAM-LW is shown in Figure 3. It is an all-reflective design with a telecentric entrance pupil and a reduction ratio of 3.

The optics is a similar system as the SW channel design with 3 mirrors (M1, M2 and M3). They are conical decentered but not critical for manufacturing.

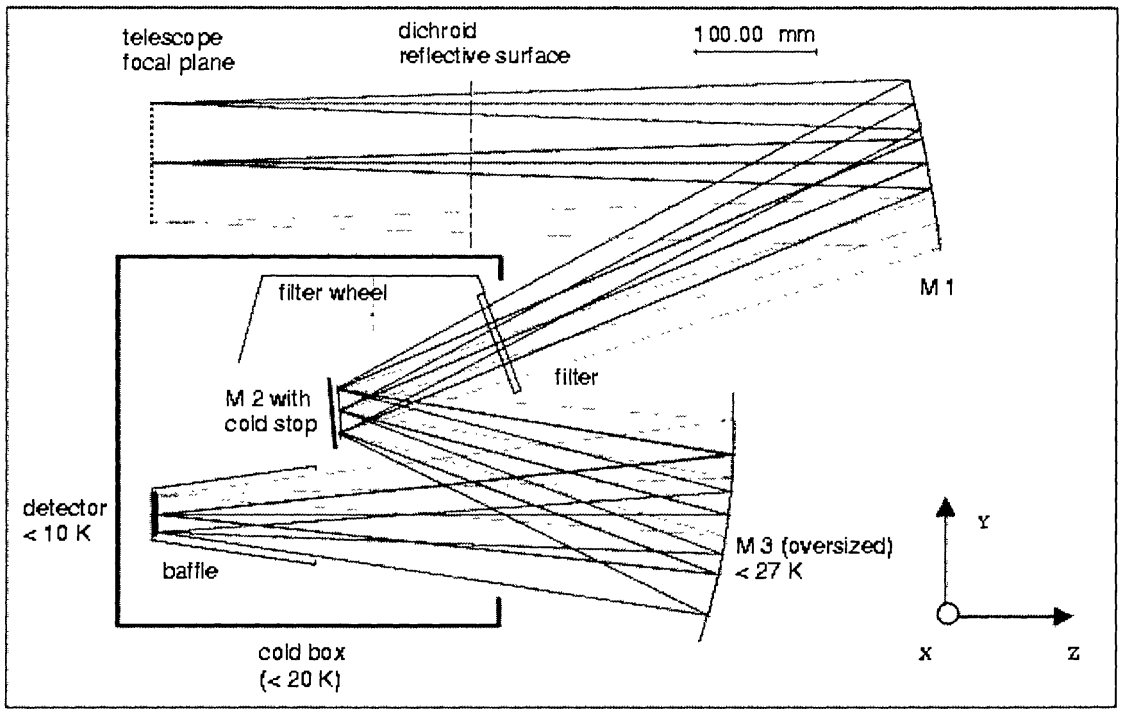

Figure 3. Optical configuration of MIRCAM-LW.

Table 2. MIRCAM: SW Design Parameters

Parameter	Value
Wavelength range	5 to 10 μm
Reduction ratio	1.5
F-number at object side	16
Field (arcmin)	$2.5' \times 2.5'$
Detector array	2K $\times$ 2K
Pixel size	30 μm (see note above)
IFOV	0.32 μrad (or 65 mas)
Entrance pupil	telecentric
Stop	at second convex mirror
Stop diameter	37 mm
Optical surfaces	2 spherical, 1 conical
Spectral Filters	Filter wheel with 6 broad band filters and one open position

The broad band filters are accommodated on a filter wheel, which is located in the parallel beam close to the pupil stop. The detector array is cooled to a temperature < 10 K. The correct image focus can be achieved by adjusting the detector array.

In the long wavelength range above 10 μm, background radiation from the sun-shield and instrument thermal self-emission will be main contributors to the

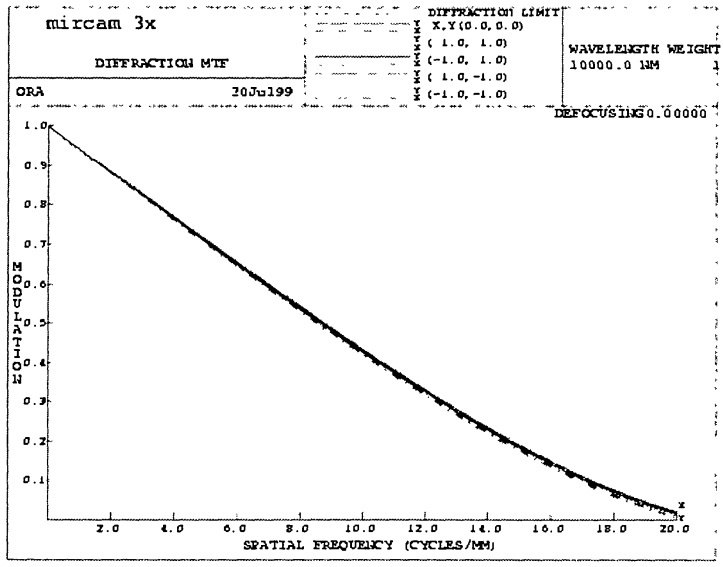

Figure 4. MIRCAM-LW: MTF as a function of spatial frequency calculated in center and corners of the field.

photon noise. The chosen configuration of the optical system allows measures to minimize these effects. All optical elements from the detector array up to and including the filters will have to be colder than the rest of the instrument. Most critical is a baffle at $\leq$ 20 K, to effectively reduce the detector field of view. M3 is oversized, so that no radiation from behind the mirror is seen by the detector. This mirror should be at a temperature below 27 K. The thermal design is schematically shown in Figure 3.

The optical performance of the camera is diffraction limited. The Strehl ratios exceed 0.99 across the whole field. The MTF as a function of frequency is given in Figure 4. The field angles are expressed in relative coordinates w.r.t. the maximum field angles.

The wavefront quality of MIRCAM-LW is better than that of MIRCAM-SW, because in MIRCAM-LW three conical mirrors are used, while in MIRCAM-SW only one conical and two spherical mirrors are used.

4. Photometric Instrument Performance

The expected in-orbit instrument performance is shown in Figure 5. The model includes all efficiencies from the telescope transmission up to the detector quantum efficiency. Background contributions include not only the zodiacal light[1] but also emission from the sunshield, scattered by the telescope prime mirror (Bély et al. 1998), and emissions from the warm and cold optics.

[1]From the NGST Exposure Time Calculator

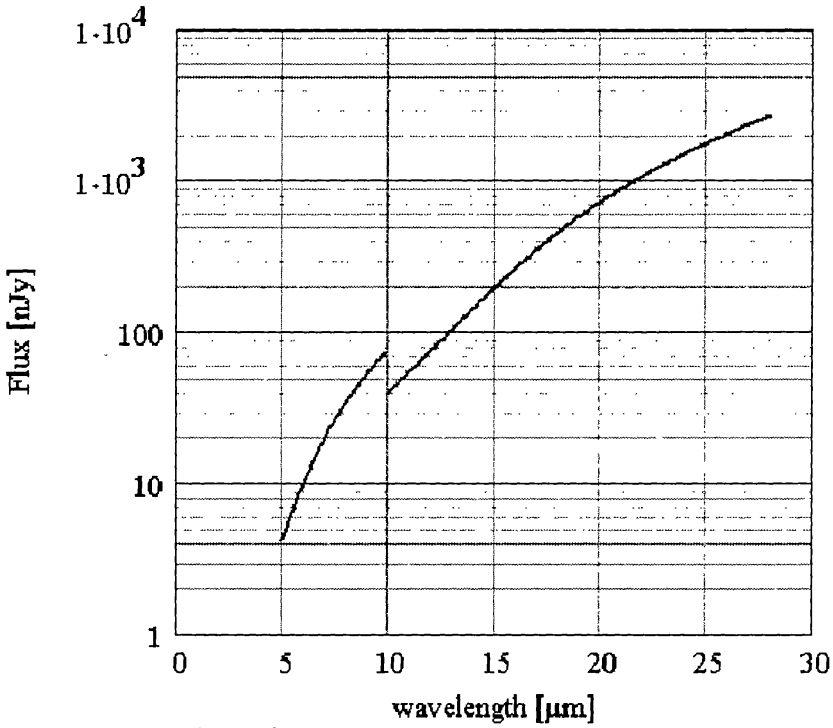

Figure 5. Flux of point sources vs. wavelength that can be resolved in the SW and LW region with an SNR of 10 and an observation time of 10^5 sec.

Table 3. MIRCAM-LW Design Parameters

Parameter	Value
Wavelength range	10 to 28 μm
Reduction ratio	3
F-number at object side	16
Field (arcmin)	$2.5' \times 2.5'$
Detector array	1K × 1K
Pixel size	30 μm (see note above)
IFOV	0.63 μrad (or 130 mas)
Entrance pupil	telecentric
Stop	at second convex mirror
Stop diameter	38 mm
Optical surfaces	3 conical
Spectral Filters	Filter wheel with 8 broad band filters in parallel beam with one open position

The performance is for all target magnitudes photon noise limited. Dominant noise sources are the zodiacal light and the scattered light from the sunshield. In case the ISIM is at < 35 K the emissions from the warm optics are negligible. The cold optics temperature of about 20 K has been selected such

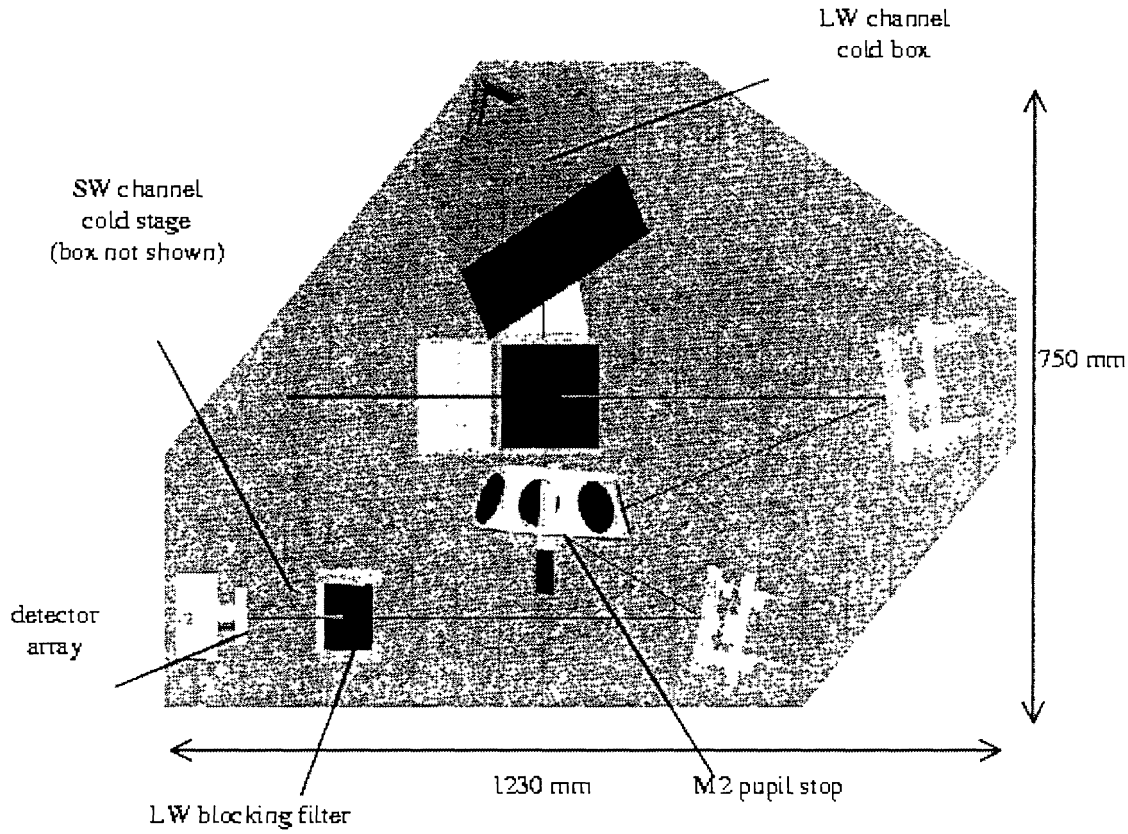

Figure 6. MIRCAM design: top view on the SW channel. The LW optical path is perpendicular to the image plane.

that this contribution will also be negligible. The detector and the readout noise are negligible for all targets.

5. Opto-Mechanical Design

The baseline opto-mechanical designs are shown in Figures 6 to 8. The optical bench as primary structure consists of a light-weighted plate made of C/SiC material. The mirrors are attached to C/SiC brackets by isostatic 3 point support. Flexible INVAR mounts are used as connection elements.

6. Conclusions

The presented mid-infrared camera design is very compact, for its large field of view. The optical performance is very good over the whole field, and thus an optimization towards an even more compact design can be envisaged (the size can be reduced by about 20% without measurable reduction in performance).

Summary of design and performance features:

+ good optical performance

+ compact overall design for the LW- and the SW-range

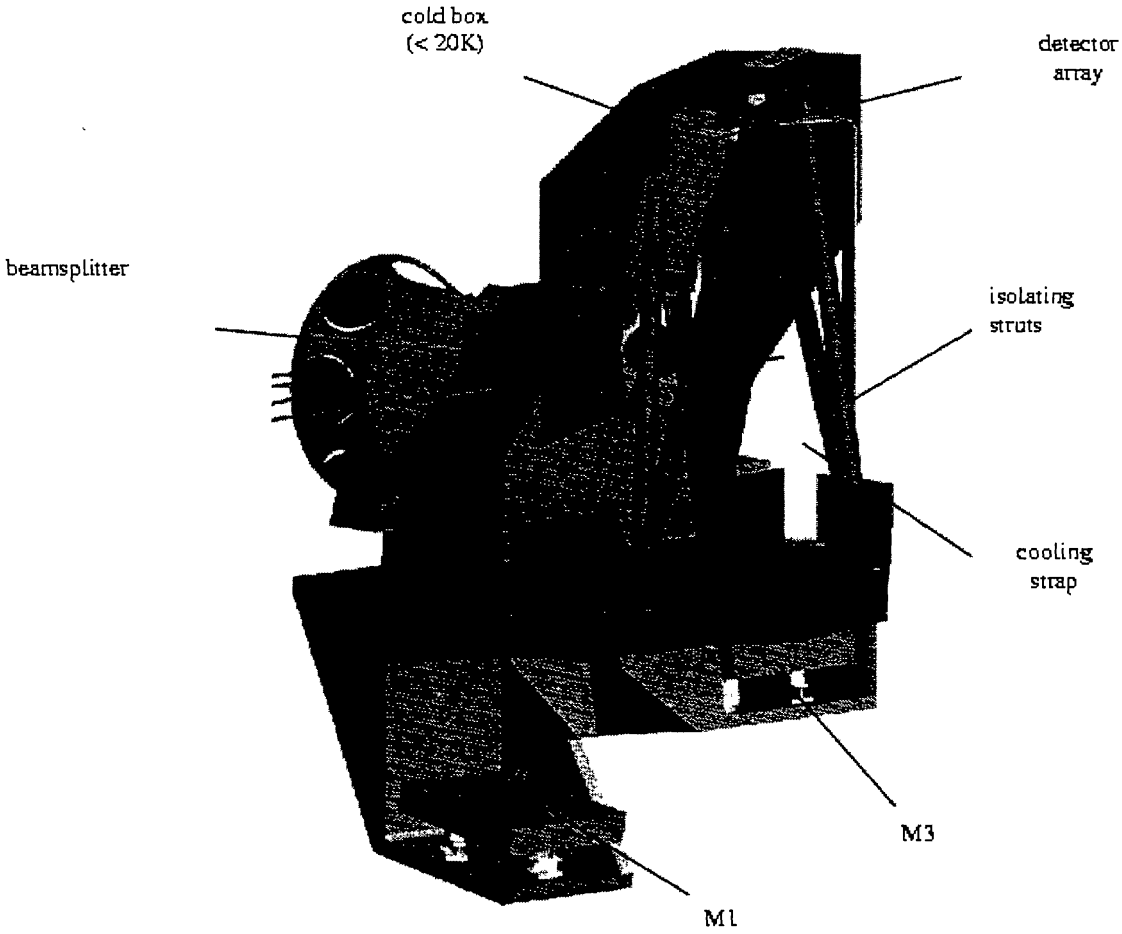

Figure 7. Close view at the LW channel with the housing partially removed. Long CFRP bars provide good thermal isolation of the cold parts.

Table 4. Estimated Instrument Budgets

Parameter	Estimated budget figure
Dimensions	$1.23 \times 0.75 \times 0.78$ m^3
Mass	45 kg (assuming C/SiC material)
Average Power (analog part only)	FPA: 1.8 mW, ASP & control: 1.85 W
Heat Load on Cooler	26 mW
Science Data Rate	100 Mbit/1000 sec
Downlink memory	4 Gbit (80 frames/day, compressed)

+ efficient cold stop in MIRCAM-LW located at the secondary mirror, that can easily be cooled

+ the thermal design guarantees a good reduction of instrument background radiation

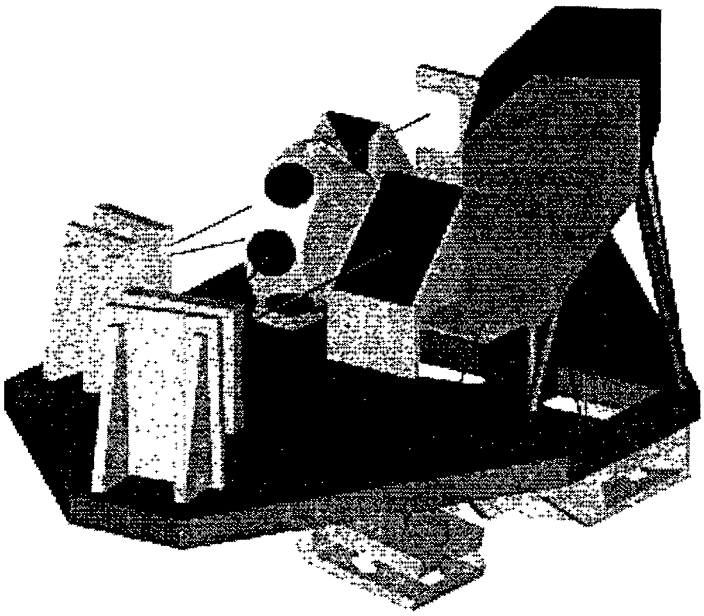

Figure 8. MIRCAM 3D view. SW channel on the left, LW channel on the right. A large dichroic in the center splits the beam.

+ filter wheel in parallel beam

– large dichroic beam-splitter

Acknowledgments. The work has been performed under ESA contract for the "Study of Payload Suite and Telescope for NGST." ESA study manager was J. Cornelisse, ESA study scientist was P. Jakobsen. We would like to particularly thank D. Elbaz, P. van der Werf, J. L. Puget and L. Vigroux for their contributions as part of the science team to the concepts presented here.

References

"Study of Payload Suite and Telescope for NGST," ESTEC/Contract No. 13111/98/NL/MS

"NGST Payload Study, Final Report," NGST-FR-DSS-PST-001, Issue 1, 22-Oct-99

Posselt, W., et al. 2000, these proceedings

Bèly, P., et al. 1998, http://www.ngst.nasa.gov/cgi-bin/doc?Id=213

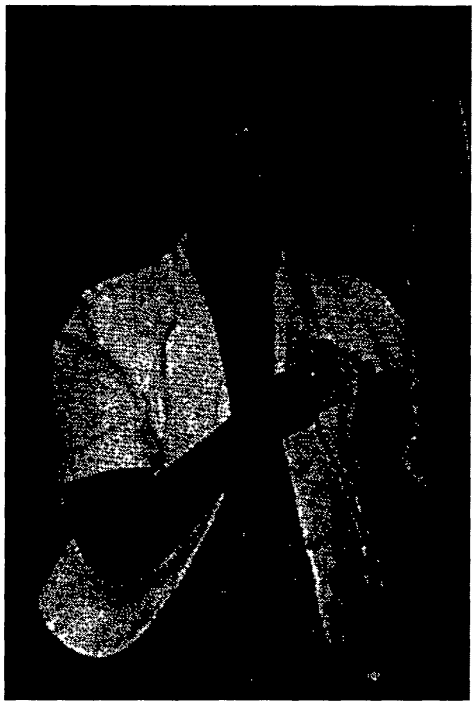

Gillian Wright